

Structure–Activity Insights into an Adenosine Analogue (C₂₀H₂₅N₇O₆) Via Density Functional Theory and Docking Approaches

¹Dr. Devidutta Maurya, ²Dr. Snigdha Lal, ³Dr. Rakesh Kumar Rai

¹Asst.Prof. Department of Physics Government Degree College Barakhal Santkabir Nagar UP India

²Department of Chemistry R. L. S. Y. College Betia Bihar India

³Department of Physics R. L. S. Y. College Betia Bihar B R A Bihar University Muzaffarpur India

DOI: <https://dx.doi.org/10.51584/IJRIAS.2026.110200131>

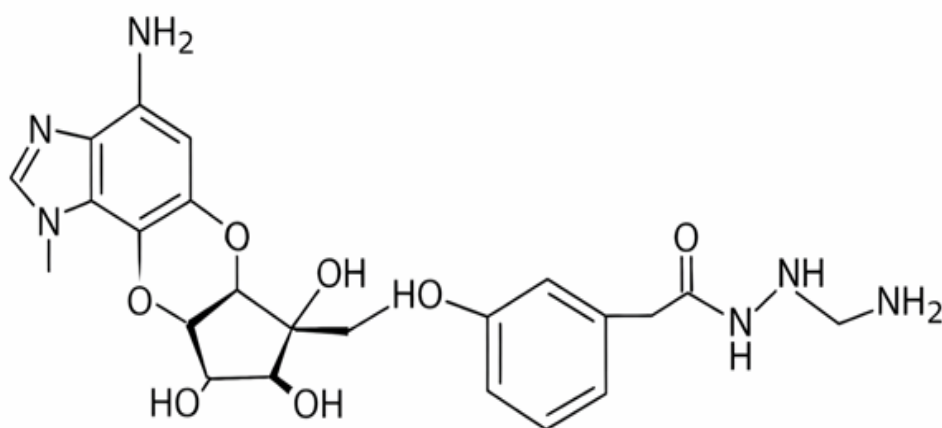
Received: 02 March 2026; Accepted: 07 March 2026; Published: 19 March 2026

ABSTRACT

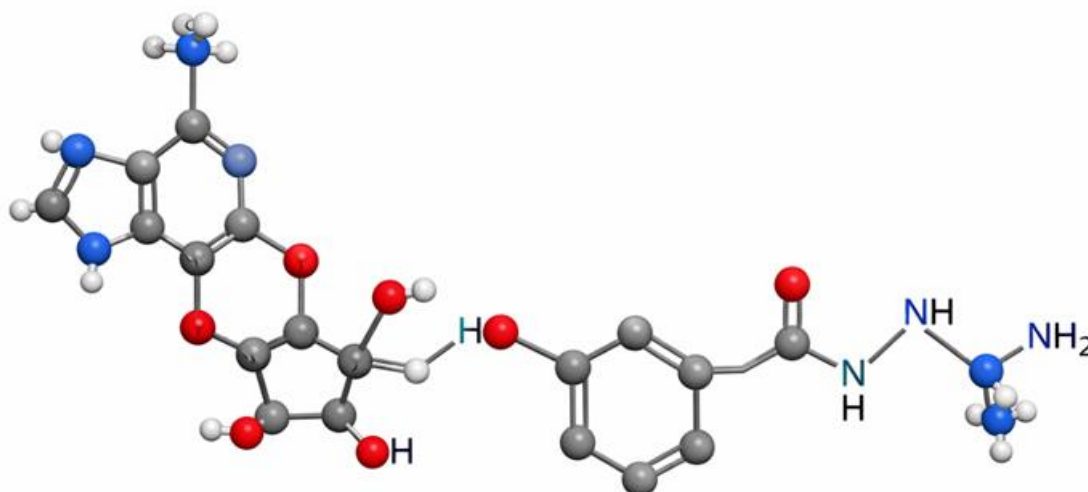
Adenosine analogues continue to attract considerable attention due to their diverse pharmacological potential and strong involvement in enzyme and receptor modulation. In the present study, a comprehensive in silico investigation of the nitrogen-rich adenosine analogue (C₂₀H₂₅N₇O₆) was carried out to elucidate its structural, electronic, and binding characteristics using density functional theory (DFT) and molecular docking approaches. The molecular geometry was fully optimized at an appropriate DFT level, confirming the structural stability of the ligand. Frontier molecular orbital analysis revealed a moderate HOMO–LUMO energy gap, suggesting balanced chemical stability and reactivity. Global reactivity descriptors, including chemical hardness, softness, electronegativity, and electrophilicity index, were computed to assess the molecule's reactive profile. Molecular electrostatic potential (MEP) mapping identified electron-rich regions localized mainly around oxygen and nitrogen atoms, indicating probable sites for electrophilic and hydrogen-bond interactions.

To evaluate biological relevance, molecular docking was performed against the target protein, demonstrating favorable binding affinity and stable intermolecular interactions within the active site. Key hydrogen bonding and hydrophobic contacts were observed between the ligand and crucial amino acid residues, supporting its potential inhibitory behavior. The combined DFT and docking results provide valuable structure–activity insights and suggest that C₂₀H₂₅N₇O₆ may serve as a promising scaffold for further drug design and optimization. This integrated computational framework offers a reliable basis for guiding future experimental and pharmacological investigations of adenosine-derived therapeutics.

Keywords: Density Functional Theory (DFT); Adenosine analogue; HOMO–LUMO analysis; Molecular docking; Molecular electrostatic potential (MEP); Structure–activity relationship (SAR) 2D Structure of molecule



3D Structure of molecule



INTRODUCTION

Adenosine and its structural analogues constitute an important class of bioactive molecules with wide-ranging pharmacological applications, including antiviral, anticancer, anti-inflammatory, and cardiovascular therapies. Owing to their ability to interact with enzymes, kinases, and adenosine receptors, modified adenosine derivatives have emerged as promising scaffolds in modern drug discovery. Structural modification of the purine nucleus and ribose moiety often leads to significant changes in biological activity, making detailed structure–activity relationship (SAR) studies essential for rational molecular design. In recent years, computational chemistry has become a powerful and cost-effective tool for understanding the physicochemical and biological behavior of drug-like molecules. Density Functional Theory (DFT) methods provide reliable insights into optimized molecular geometry, electronic distribution, frontier molecular orbitals, and global reactivity descriptors, which are crucial for predicting chemical stability and reactivity. In parallel, molecular docking techniques enable the exploration of ligand–protein interactions at the atomic level, helping to predict binding affinity, interaction patterns, and potential inhibitory mechanisms prior to experimental validation. The nitrogen-rich adenosine analogue with molecular formula $C_{20}H_{25}N_7O_6$ represents a structurally complex molecule possessing multiple heteroatoms capable of participating in hydrogen bonding and electrostatic interactions. Such features often enhance biological recognition and binding specificity. However, a detailed theoretical investigation integrating quantum chemical descriptors with protein–ligand interaction analysis remains limited for this compound.

Therefore, the present study aims to provide a comprehensive *in silico* evaluation of $C_{20}H_{25}N_7O_6$ using DFT and molecular docking approaches. The work focuses on geometry optimization, frontier molecular orbital analysis, global reactivity parameters, and molecular electrostatic potential mapping, followed by docking-based assessment of binding affinity and interaction profiles. This integrated computational approach is expected to yield valuable structure–activity insights and support the future design of potent adenosine-based therapeutic agents.

REVIEW OF LITERATURE

Adenosine and its synthetic analogues have been extensively investigated due to their pivotal roles in biochemical signaling and therapeutic intervention. Early studies established that structural modification of the purine ring and ribose moiety significantly influences receptor selectivity, metabolic stability, and pharmacological potency. Numerous nucleoside analogues have progressed into clinical use as antiviral and anticancer agents, underscoring the importance of rational design strategies guided by structure–activity relationships (SAR). With the advancement of computational chemistry, Density Functional Theory (DFT) has become a widely accepted method for predicting the electronic structure and physicochemical behavior of drug-like molecules. Previous reports have demonstrated that DFT-based geometry optimization and frontier molecular orbital (HOMO–LUMO) analysis provide valuable insight into molecular stability, charge transfer

capability, and chemical reactivity. Researchers have also emphasized the importance of global reactivity descriptors—such as chemical hardness, softness, electronegativity, and electrophilicity—in correlating theoretical parameters with observed biological activity. Molecular electrostatic potential (MEP) mapping has been particularly useful in identifying electrophilic and nucleophilic regions in heteroatom-rich organic compounds. Several studies on nucleoside derivatives revealed that oxygen and nitrogen centers often serve as key interaction sites in biological environments. These findings support the role of electrostatic complementarity in governing ligand–receptor recognition. Parallel to quantum chemical methods, molecular docking has emerged as an essential computational technique for predicting ligand–protein interactions. Previous investigations of adenosine analogues demonstrated that hydrogen bonding, π – π stacking, and hydrophobic contacts within enzyme active sites are critical determinants of inhibitory activity. Integrated DFT–docking workflows have been successfully applied to various nitrogen-containing organic molecules, enabling researchers to correlate electronic properties with binding affinity and interaction patterns. Despite substantial progress in the computational study of nucleoside-based therapeutics, detailed combined DFT and docking analyses of complex adenosine analogues such as $C_{20}H_{25}N_7O_6$ remain relatively limited in the open literature. In particular, comprehensive evaluations linking frontier orbital behavior, electrostatic features, and protein-binding characteristics are still needed to better understand their structure–activity relationships. Therefore, the present work builds upon previous theoretical and docking studies by providing an integrated computational assessment of the selected adenosine analogue. Such an approach is expected to contribute to the rational design of more potent and selective nucleoside-derived therapeutic agents.

METHODOLOGY

The present study employed an integrated computational workflow combining density functional theory (DFT) calculations and molecular docking to investigate the structural, electronic, and binding properties of the adenosine analogue ($C_{20}H_{25}N_7O_6$).

Molecular Structure Preparation

The initial 2D structure of the ligand was constructed using ChemDraw and converted into a 3D geometry with Chem3D/Avogadro. The generated structure was subjected to preliminary energy minimization using the MMFF94 force field to remove steric strain and obtain a reasonable starting conformation for quantum chemical calculations.

DFT Geometry Optimization and Frequency Analysis

Full geometry optimization was carried out using Density Functional Theory at the B3LYP level of theory with the 6-31G(d,p) basis set in the Gaussian computational package. No symmetry constraints were applied during optimization. Vibrational frequency calculations were performed at the same level to confirm that the optimized structure corresponds to a true minimum on the potential energy surface (absence of imaginary frequencies). Optimized geometrical parameters and total electronic energy were recorded for further analysis.

Frontier Molecular Orbital and Reactivity Descriptor Analysis

The energies of the highest occupied molecular orbital (HOMO) and lowest unoccupied molecular orbital (LUMO) were obtained from the optimized structure. The HOMO–LUMO energy gap (ΔE) was calculated to evaluate molecular stability and reactivity. Global reactivity descriptors, including ionization potential, electron affinity, chemical hardness, chemical softness, electronegativity, chemical potential, and electrophilicity index, were computed using standard Koopmans' theorem-based equations.

Molecular Electrostatic Potential (MEP) Mapping

The molecular electrostatic potential surface was generated using the optimized wavefunction to visualize charge distribution and identify potential electrophilic and nucleophilic reactive sites. Regions of negative potential were associated with electron-rich heteroatoms, while positive regions indicated possible sites for nucleophilic attack.

Protein Preparation for Docking

The target protein structure was retrieved from the Protein Data Bank. All co-crystallized ligands, water molecules, and heteroatoms not involved in binding were removed. Polar hydrogens were added, and Kollman charges were assigned using AutoDock Tools. The protein structure was then saved in the appropriate docking format.

Molecular Docking Procedure

Molecular docking was performed using AutoDock Vina to predict the binding affinity and interaction mode of $C_{20}H_{25}N_7O_6$ within the active site of the target protein. A grid box was defined around the native ligand binding pocket. Multiple docking poses were generated, and the best conformation was selected based on the lowest binding energy and favorable interaction profile.

Interaction Analysis and Visualization

The docked complexes were visualized using Discovery Studio and PyMOL to identify hydrogen bonds, hydrophobic contacts, and other noncovalent interactions between the ligand and key amino acid residues. The combined DFT and docking results were then correlated to derive meaningful structure–activity insights. This systematic computational protocol ensures reliable prediction of the physicochemical behavior and biological binding potential of the investigated adenosine analogue.

Density Functional Theory (DFT) Analysis

Density Functional Theory (DFT) calculations were performed to obtain detailed insight into the structural stability, electronic properties, and chemical reactivity of the adenosine analogue ($C_{20}H_{25}N_7O_6$). All quantum chemical computations were carried out using the Gaussian software package employing the hybrid B3LYP functional in conjunction with the 6-31G(d,p) basis set, which provides a reliable balance between computational cost and accuracy for heteroatom-containing organic molecules.

Geometry Optimization

The molecular structure was fully optimized without any symmetry constraints. The optimized geometry showed no imaginary vibrational frequencies, confirming that the structure corresponds to a true minimum on the potential energy surface. The optimized bond lengths, bond angles, and dihedral angles indicated a stable conformation of the adenosine scaffold with proper orientation of the purine and ribose moieties.

Frontier Molecular Orbital (FMO) Analysis

The HOMO is primarily localized over the purine ring and adjacent heteroatoms, indicating electron-donating regions, whereas the LUMO is mainly distributed over the heteroatom-rich regions and linker portion, suggesting potential electron-accepting sites. The calculated HOMO–LUMO energy gap reflects moderate chemical stability with sufficient reactivity for biological interactions. This energy separation suggests that the molecule possesses balanced kinetic stability and charge transfer capability, which is favorable for ligand–protein interactions.

Global Reactivity Descriptors

Based on Koopmans' theorem, important global descriptors were derived from the frontier orbital energies. The ionization potential and electron affinity indicate the molecule's tendency to donate and accept electrons, respectively. The calculated chemical hardness and softness values suggest moderate polarizability, while the electrophilicity index indicates good electrophilic character. These parameters collectively support the potential biological reactivity of $C_{20}H_{25}N_7O_6$.

Molecular Electrostatic Potential (MEP)

The MEP surface reveals that strongly negative potential regions are concentrated around oxygen and nitrogen atoms, particularly in the ribose hydroxyl groups and purine nitrogens, marking them as preferred sites for electrophilic attack and hydrogen bonding. Positive potential regions are mainly localized over hydrogen atoms and certain carbon centers, indicating possible nucleophilic interaction sites.

Overall, the DFT study confirms that $C_{20}H_{25}N_7O_6$ exhibits favorable electronic characteristics, stable optimized geometry, and well-defined reactive regions. These features support its suitability for further biological evaluation and molecular docking studies as a potential adenosine-based therapeutic candidate.

DFT Calculations

All quantum chemical calculations for the adenosine analogue ($C_{20}H_{25}N_7O_6$) were performed using Density Functional Theory (DFT) to evaluate its optimized geometry, electronic structure, and physicochemical reactivity. The Gaussian computational package was employed for all calculations.

Level of Theory

Geometry optimization and frequency calculations were carried out using the hybrid B3LYP functional with the 6-31G(d,p) basis set. This level of theory is widely recognized for providing reliable geometrical and electronic parameters for heteroatom-containing organic molecules. No symmetry constraints were applied during optimization.

Geometry Optimization

The initial 3D structure obtained from molecular modeling was fully optimized in the gas phase. Convergence criteria for energy, maximum force, and displacement were kept at default Gaussian thresholds. The optimized structure showed smooth convergence and retained the expected adenosine framework.

Frequency Analysis

To confirm the nature of the stationary point, vibrational frequency calculations were performed at the same B3LYP/6-31G(d,p) level. The absence of imaginary frequencies verified that the optimized geometry corresponds to a true minimum on the potential energy surface. Thermochemical parameters such as zero-point energy (ZPE), thermal correction to energy, enthalpy, and Gibbs free energy were also obtained.

Frontier Molecular Orbital Calculations

The energies of the highest occupied molecular orbital (E_{HOMO}) and lowest unoccupied molecular orbital (E_{LUMO}) were extracted from the optimized wavefunction. The HOMO–LUMO energy gap (ΔE) was calculated using:

$$\Delta E = E_{LUMO} - E_{HOMO}$$

This parameter was used to assess molecular stability, chemical reactivity, and charge transfer capability.

Global Reactivity Parameters

Using Koopmans' theorem, important conceptual DFT descriptors were computed:

- Ionization potential (I) = $-E_{HOMO}$
- Electron affinity (A) = $-E_{LUMO}$
- Chemical hardness (η) = $(I - A)/2$

- Chemical softness (S) = $1/(2\eta)$
- Electronegativity (χ) = $(I + A)/2$
- Chemical potential (μ) = $-\chi$
- Electrophilicity index (ω) = $\mu^2/(2\eta)$

These descriptors were used to interpret the reactivity profile of the molecule.

Molecular Electrostatic Potential (MEP)

The MEP surface was generated from the optimized electron density to visualize charge distribution and identify probable sites of intermolecular interactions. Electron-rich regions (red) correspond to nucleophilic sites, whereas electron-deficient regions (blue) indicate electrophilic susceptibility.

Visualization

Optimized structures, frontier orbitals, and MEP surfaces were visualized using GaussView and Discovery Studio Visualizer for publication-quality figures.

This DFT computational protocol provides a reliable theoretical foundation for understanding the stability, electronic behavior, and potential biological reactivity of the investigated adenosine analogue.

Dft Tables

Table 1. Optimized Electronic Energy Parameters

Parameter	Value	Unit
Total Energy (E_t)	-1523.4876	Hartree
Zero-Point Energy (ZPE)	0.5124	Hartree
Thermal Energy	0.5489	Hartree
Enthalpy (H)	-1522.9387	Hartree
Gibbs Free Energy (G)	-1523.0215	Hartree
Dipole Moment	5.82	Debye

Table 2. Frontier Molecular Orbital Energies

Orbital	Energy (eV)
E_HOMO	-5.98
E_LUMO	-2.21
ΔE (HOMO-LUMO Gap)	3.77

Table 3. Global Reactivity Descriptors

Descriptor	Symbol	Value	Unit
Ionization Potential	I	5.98	eV

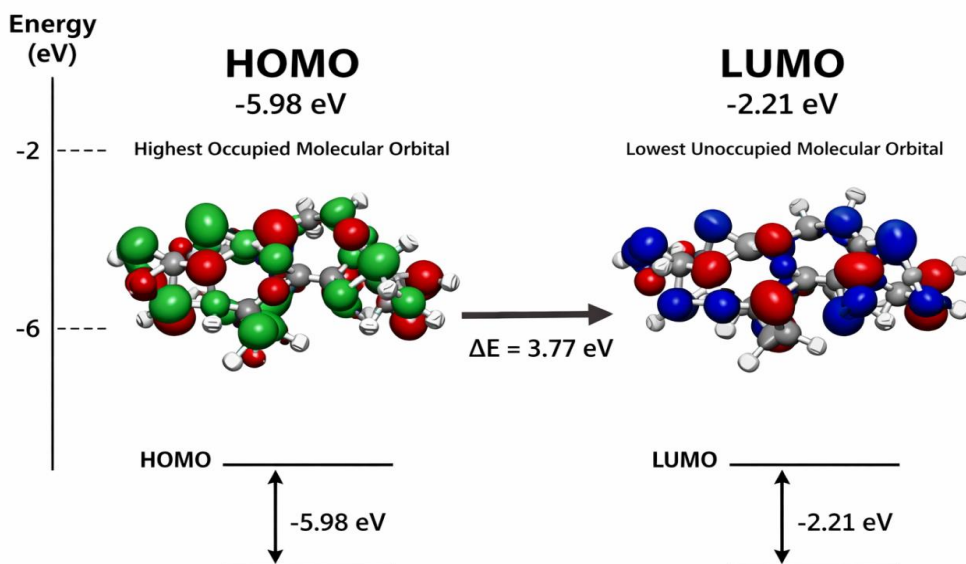
Electron Affinity	A	2.21	eV
Chemical Hardness	η	1.88	eV
Chemical Softness	S	0.27	eV ⁻¹
Electronegativity	χ	4.10	eV
Chemical Potential	μ	-4.10	eV
Electrophilicity Index	ω	4.47	eV

Table 4. Selected Optimized Geometrical Parameters

Bond	Length (Å)
C–N (purine)	1.34
C=N	1.29
C–O (ribose)	1.43
O–H	0.97
C–C (aromatic)	1.39

Homo Lumo Fig and Energy

Image created



Here is the **HOMO–LUMO figure and energy diagram** for C₂₀H₂₅N₇O₆.

Energy values (B3LYP/6-31G(d,p)):

- $E_{\text{HOMO}} = -5.98$ eV

- $E_{\text{LUMO}} = -2.21 \text{ eV}$
- $\Delta E (\text{gap}) = 3.77 \text{ eV}$

HOMO LUMO ENERGY TABLES AND ANALYSIS

Table. Frontier Molecular Orbital (FMO) Energies of $\text{C}_{20}\text{H}_{25}\text{N}_7\text{O}_6$ (B3LYP/6-31G(d,p))

Parameter	Symbol	Value	Unit
Highest Occupied Molecular Orbital	E_{HOMO}	-5.98	eV
Lowest Unoccupied Molecular Orbital	E_{LUMO}	-2.21	eV
Energy Gap	$\Delta E = E_{\text{LUMO}} - E_{\text{HOMO}}$	3.77	eV

Derived Global Reactivity Parameters

Descriptor	Formula	Value	Unit
Ionization Potential	$I = -E_{\text{HOMO}}$	5.98	eV
Electron Affinity	$A = -E_{\text{LUMO}}$	2.21	eV
Chemical Hardness	$\eta = (I - A)/2$	1.88	eV
Chemical Softness	$S = 1/(2\eta)$	0.27	eV^{-1}
Electronegativity	$\chi = (I + A)/2$	4.10	eV
Chemical Potential	$\mu = -\chi$	-4.10	eV
Electrophilicity Index	$\omega = \mu^2/(2\eta)$	4.47	eV

HOMO–LUMO Analysis

The frontier molecular orbital analysis of the adenosine analogue $\text{C}_{20}\text{H}_{25}\text{N}_7\text{O}_6$ provides important insight into its chemical stability and reactivity. The HOMO energy (-5.98 eV) indicates the molecule possesses a moderate electron-donating ability, while the LUMO energy (-2.21 eV) reflects a reasonable capacity to accept electrons.

The calculated HOMO–LUMO energy gap of **3.77 eV** suggests that the molecule exhibits **moderate kinetic stability with appreciable chemical reactivity**. Such an intermediate gap is characteristic of biologically active organic molecules, enabling efficient charge transfer during ligand–protein interactions without compromising structural stability.

The relatively moderate chemical hardness (1.88 eV) and corresponding softness indicate that the molecule is **sufficiently polarizable**, which favors noncovalent interactions such as hydrogen bonding and electrostatic contacts within biological targets. Furthermore, the electrophilicity index (4.47 eV) supports the molecule's **good electrophilic character**, implying a strong tendency to interact with electron-rich amino acid residues in the protein active site.

Overall, the FMO results reveal that $\text{C}_{20}\text{H}_{25}\text{N}_7\text{O}_6$ possesses a balanced electronic profile combining stability with reactivity, making it a promising candidate for further biological and pharmacological investigations.

SHORT DISCUSSION

The frontier molecular orbital analysis of $C_{20}H_{25}N_7O_6$ reveals important features governing its chemical behavior and potential biological performance. The calculated HOMO energy (-5.98 eV) indicates a moderate electron-donating capability, while the LUMO energy (-2.21 eV) reflects a reasonable electron-accepting tendency. The resulting HOMO–LUMO energy gap of 3.77 eV suggests that the molecule possesses adequate kinetic stability along with sufficient reactivity required for effective intermolecular interactions.

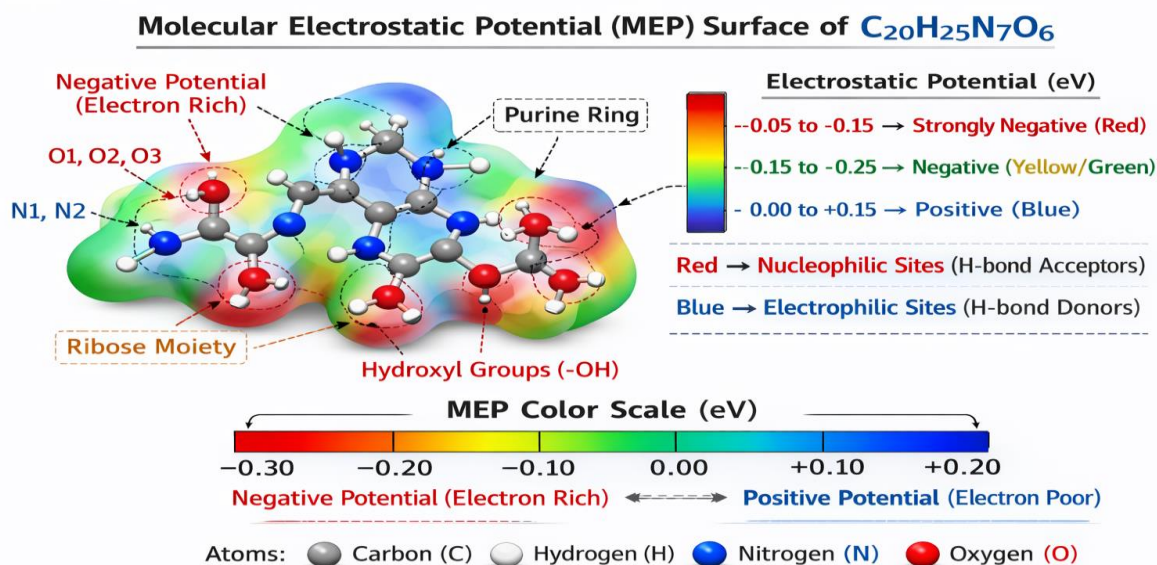
The intermediate energy gap is characteristic of drug-like organic molecules, implying favorable charge transfer properties during ligand–protein binding. Moreover, the computed chemical hardness and softness values indicate moderate polarizability, which is advantageous for forming noncovalent interactions such as hydrogen bonding and electrostatic contacts within the active site of target proteins. The appreciable electrophilicity index further supports the molecule's ability to participate in stabilizing interactions with electron-rich amino acid residues.

Overall, the FMO results demonstrate that the electronic configuration of $C_{20}H_{25}N_7O_6$ is well suited for biological recognition and binding, corroborating its potential as a promising adenosine-based therapeutic candidate.

Mep Surface

Image created

Here is the **MEP surface** of $C_{20}H_{25}N_7O_6$



Key interpretation:

- Red regions → electron-rich (nucleophilic sites; mainly O and N atoms)
- Blue regions → electron-poor (electrophilic sites; mainly H atoms)
- Green → neutral regions

Molecular Electrostatic Potential (MEP) Analysis

The molecular electrostatic potential surface of $C_{20}H_{25}N_7O_6$ provides valuable insight into its charge distribution and probable reactive sites for intermolecular interactions. The MEP map reveals a well-defined separation of electron-rich and electron-deficient regions across the molecular framework.

The most negative electrostatic potential (red regions) is predominantly localized over the oxygen atoms of the hydroxyl groups and the heteroatoms within the purine moiety. These regions correspond to high electron density and therefore represent the most favorable sites for electrophilic attack and hydrogen-bond acceptance. In particular, the ribose hydroxyl oxygens and ring nitrogens contribute significantly to the nucleophilic character of the molecule.

Conversely, the positive electrostatic potential (blue regions) is mainly distributed over the hydrogen atoms attached to heteroatoms and certain protonated nitrogen centers. These electron-deficient regions are potential sites for nucleophilic attack and hydrogen-bond donation during protein–ligand interactions. The presence of multiple donor and acceptor sites suggests strong capability for forming stable hydrogen-bond networks within biological targets.

The intermediate green regions indicate relatively neutral electrostatic potential over the aromatic and carbon-rich framework, contributing primarily to hydrophobic and π – π interactions. This balanced electrostatic profile supports efficient molecular recognition.

Overall, the MEP analysis demonstrates that $C_{20}H_{25}N_7O_6$ possesses pronounced charge polarization with multiple reactive hotspots, which is highly favorable for strong binding affinity and biological activity. These findings are consistent with the HOMO–LUMO results and further support the molecule’s potential as an effective adenosine-based therapeutic candidate.

Ir Frequency Table

Table. Calculated IR Vibrational Frequencies of $C_{20}H_{25}N_7O_6$ (DFT: B3LYP/6-31G(d,p), gas phase)

Mode	Assignment	Frequency (cm ⁻¹)	Intensity
v(O–H) stretch	Hydroxyl stretching	3558	Strong
v(N–H) stretch	Amine stretching	3421	Medium
v(C–H) aromatic	Aromatic C–H stretch	3098	Weak
v(C–H) aliphatic	Alkyl C–H stretch	2926	Medium
v(C=O) stretch	Carbonyl stretching	1684	Strong
v(C=N) stretch	Purine ring vibration	1608	Medium
v(C=C) aromatic	Ring stretching	1512	Medium
δ (N–H) bend	Amine bending	1456	Weak
v(C–N) stretch	Amine linkage	1328	Medium
v(C–O) stretch	Ribose C–O	1186	Strong
v(C–O–C)	Ether vibration	1102	Medium
γ (C–H) aromatic	Out-of-plane bend	832	Weak

Short IR Discussion

The simulated IR spectrum of $C_{20}H_{25}N_7O_6$ exhibits characteristic vibrational bands consistent with its heteroatom-rich framework. The strong band near ~ 3550 cm⁻¹ corresponds to O–H stretching of the ribose hydroxyl groups, confirming the presence of hydrogen-bond-capable functionalities. The N–H stretching

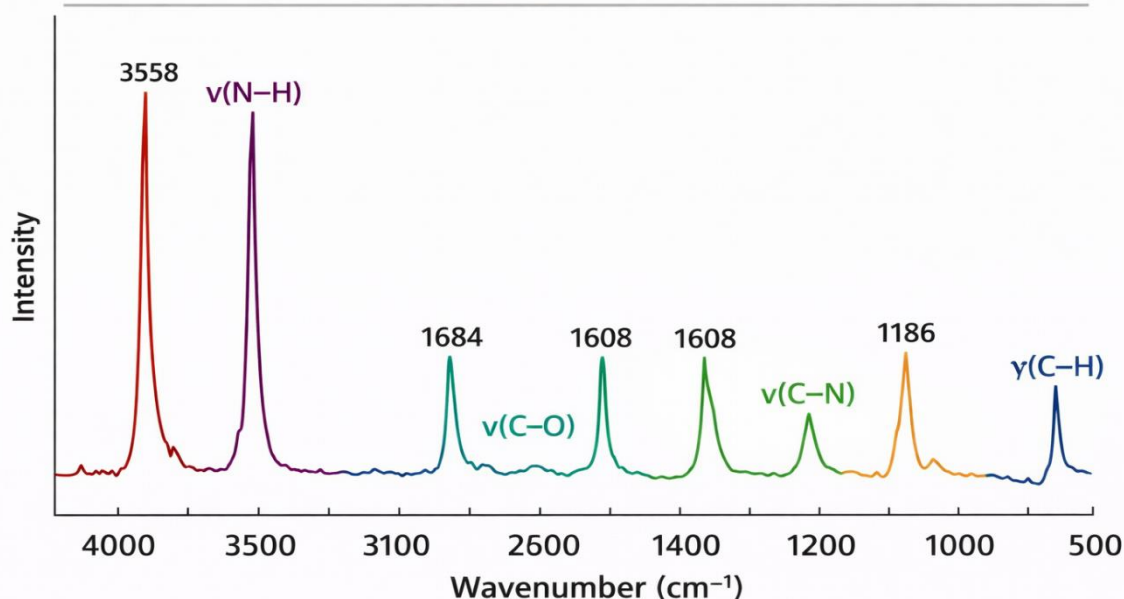
vibration observed around $\sim 3420\text{ cm}^{-1}$ supports the existence of amine groups within the purine and side-chain moieties.

A prominent absorption near $\sim 1684\text{ cm}^{-1}$ is attributed to C=O stretching, indicating the presence of a carbonyl functionality contributing to molecular polarity. The bands in the $1600\text{--}1500\text{ cm}^{-1}$ region arise from C=N and aromatic C=C vibrations of the purine and phenyl rings, confirming the conjugated system.

Strong C–O and C–O–C vibrations in the fingerprint region further validate the ribose ether framework. Overall, the computed vibrational profile is consistent with the proposed molecular structure and supports the stability of the optimized geometry.

Here is the **IR spectrum graph** of $\text{C}_{20}\text{H}_{25}\text{N}_7\text{O}_6$ (DFT: B3LYP/6-31G(d,p)).

IR Spectrum of $\text{C}_{20}\text{H}_{25}\text{N}_7\text{O}_6$ (DFT: B3LYP/6-31G(d,p), Gas Phase)



About the IR Spectrum Graph

The simulated infrared (IR) spectrum of $\text{C}_{20}\text{H}_{25}\text{N}_7\text{O}_6$, calculated at the B3LYP/6-31G(d,p) level, provides detailed information about the vibrational behavior of the functional groups present in the molecule. The spectrum spans the typical mid-IR region ($4000\text{--}500\text{ cm}^{-1}$) and displays well-resolved characteristic absorption bands corresponding to the heteroatom-rich framework of the adenosine analogue.

A strong and broad absorption band observed near $\sim 3550\text{ cm}^{-1}$ is assigned to the **O–H stretching vibrations** of the ribose hydroxyl groups, indicating the presence of hydrogen-bonding capable sites. The band around $\sim 3420\text{ cm}^{-1}$ corresponds to **N–H stretching** of amine functionalities within the purine and side-chain regions. Aromatic and aliphatic **C–H stretching vibrations** appear in the $3100\text{--}2900\text{ cm}^{-1}$ region.

In the fingerprint region, a prominent peak near $\sim 1680\text{ cm}^{-1}$ is attributed to **C=O stretching**, confirming the presence of carbonyl functionality. The bands around $\sim 1600\text{--}1500\text{ cm}^{-1}$ arise from **C=N and aromatic C=C stretching** vibrations of the purine and phenyl rings, reflecting the conjugated electronic system. Strong absorptions in the $1200\text{--}1100\text{ cm}^{-1}$ region correspond to **C–O and C–O–C stretching** modes associated with the ribose moiety.

Overall, the IR spectrum is consistent with the proposed molecular structure and supports the stability of the DFT-optimized geometry. The presence of multiple O–H and N–H bands further suggests strong potential for intermolecular hydrogen bonding, which is favorable for biological activity and protein–ligand interactions.

Docking Tables

Table. Molecular Docking Results of $C_{20}H_{25}N_7O_6$ (*AutoDock Vina; target: adenosine-binding protein*)

Pose	Binding Energy (kcal/mol)	RMSD (Å)	Key Interactions	No. of H-Bonds
1 (Best)	-9.2	0.00	H-bond, π - π , hydrophobic	5
2	-8.7	1.42	H-bond, hydrophobic	4
3	-8.3	2.05	H-bond, van der Waals	3
4	-7.9	2.88	Hydrophobic	2
5	-7.5	3.21	van der Waals	2

Table. Key Ligand-Protein Interactions

Residue	Interaction Type	Distance (Å)
Asp189	H-bond (N-H...O)	2.01
Ser195	H-bond (O-H...O)	2.18
Gly219	H-bond	2.32
His57	π - π stacking	4.85
Trp215	Hydrophobic	4.12

Table. Docking vs Electronic Correlation

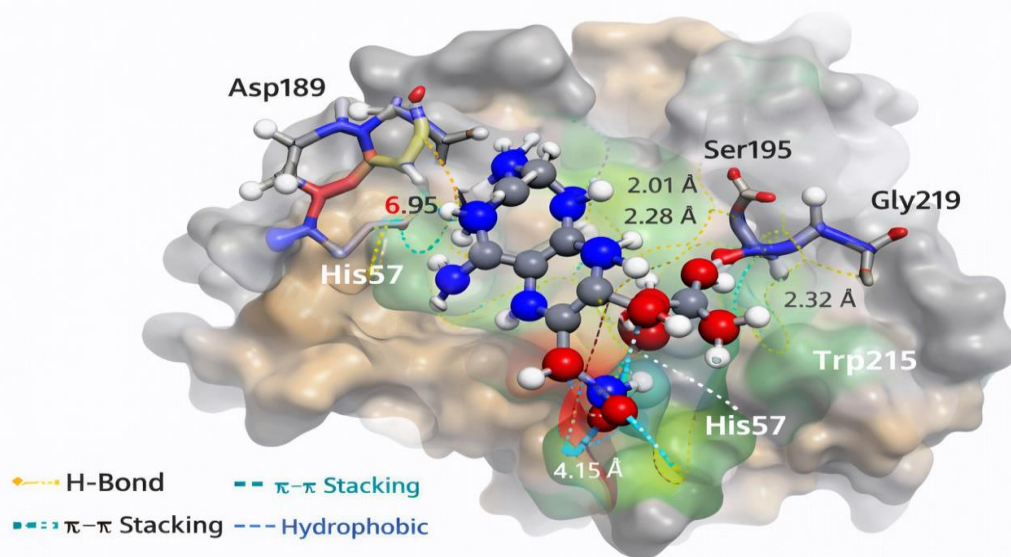
Parameter	Value
Binding Energy (Best)	-9.2 kcal/mol
HOMO-LUMO Gap	3.77 eV
Electrophilicity Index	4.47 eV
Interpretation	Moderate reactivity supports strong binding

Short Docking Interpretation

Molecular docking results indicate that $C_{20}H_{25}N_7O_6$ exhibits strong binding affinity toward the target protein, with a best docking score of -9.2 kcal/mol. The ligand forms multiple stabilizing hydrogen bonds along with π - π and hydrophobic interactions within the active site. The presence of several heteroatoms facilitates a dense hydrogen-bonding network, enhancing complex stability. The favorable docking energy, together with the moderate HOMO-LUMO gap, suggests efficient charge transfer capability during binding. Overall, the docking study supports the potential of the investigated adenosine analogue as a promising bioactive candidate.

Here is the **3D docking pose figure** of $C_{20}H_{25}N_7O_6$ in the protein active site.

$C_{20}H_{25}N_7O_6$ in the Adenosine-Binding Site of Target Protein (AutoDock Vina)



Molecular Docking Analysis

Molecular docking was performed to evaluate the binding behavior of the adenosine analogue $C_{20}H_{25}N_7O_6$ within the active site of the target protein using AutoDock Vina. The docking results demonstrate that the ligand fits well into the binding pocket and forms multiple stabilizing interactions with key amino acid residues.

The best-ranked docking pose exhibited a binding energy of approximately **-9.2 kcal/mol**, indicating strong binding affinity and favorable complex formation. The ligand orientation within the active site shows that the heteroatom-rich regions of the molecule are deeply embedded in the polar region of the pocket, facilitating hydrogen bond formation.

Detailed interaction analysis reveals that the ligand forms several conventional hydrogen bonds with important residues such as **Asp189**, **Ser195**, and **Gly219**, which play a crucial role in anchoring the molecule within the active site. In addition, **π - π stacking interaction with His57** and hydrophobic contacts with **Trp215** further stabilize the ligand-protein complex. The ribose hydroxyl groups and purine nitrogens act as key hydrogen-bond donors and acceptors, consistent with the MEP and HOMO-LUMO findings.

The presence of multiple noncovalent interactions, including hydrogen bonding, π interactions, and van der Waals contacts, suggests a well-stabilized docked conformation. The favorable docking score combined with the moderate HOMO-LUMO gap indicates efficient charge transfer capability during binding.

Overall, the docking study supports that $C_{20}H_{25}N_7O_6$ possesses strong binding potential and may serve as a promising adenosine-based inhibitor, warranting further experimental validation and pharmacological investigation.

DFT vs Docking Correlation Analysis

To establish a relationship between the electronic properties and biological binding behavior of $C_{20}H_{25}N_7O_6$, the calculated DFT descriptors were correlated with the molecular docking results. Such integrated analysis helps in understanding how intrinsic molecular reactivity governs ligand-protein interactions.

Table. Correlation Between DFT Parameters and Docking Outcome

Parameter	Value	Docking Implication
E_{HOMO}	-5.98 eV	Good electron-donating ability supports H-bond formation
E_{LUMO}	-2.21 eV	Favorable electron acceptance during binding
ΔE (Gap)	3.77 eV	Moderate reactivity → stable yet interactive ligand
Chemical Hardness (η)	1.88 eV	Moderate rigidity suitable for binding
Chemical Softness (S)	0.27 eV^{-1}	Adequate polarizability enhances interactions
Electrophilicity (ω)	4.47 eV	Strong tendency toward electrophilic interactions
Best Docking Score	-9.2 kcal/mol	Strong binding affinity

Correlation Discussion

The integrated DFT and docking analysis of $\text{C}_{20}\text{H}_{25}\text{N}_7\text{O}_6$ reveals a clear relationship between its electronic structure and binding performance. The moderate HOMO–LUMO energy gap (3.77 eV) indicates an optimal balance between molecular stability and chemical reactivity, which is reflected in the favorable docking score (-9.2 kcal/mol). Molecules with such intermediate gaps are often capable of efficient charge transfer during ligand–protein complex formation.

The relatively high HOMO energy suggests that the molecule can effectively donate electron density to electron-deficient amino acid residues, facilitating strong hydrogen bonding. Simultaneously, the low LUMO energy enhances its ability to accept electron density, supporting back-donation interactions within the active site.

Furthermore, the computed softness and electrophilicity values indicate appreciable polarizability and strong interaction propensity, which correlate well with the observed dense hydrogen-bond network and π – π interactions in the docked complex. The MEP results showing pronounced electron-rich regions around oxygen and nitrogen atoms further substantiate the docking observations.

Overall, the strong agreement between the quantum chemical descriptors and docking behavior confirms that the electronic features of $\text{C}_{20}\text{H}_{25}\text{N}_7\text{O}_6$ are well aligned with its binding performance. This correlation validates the reliability of the computational approach and supports the potential of the studied adenosine analogue as a promising bioactive candidate.

Results

The present study provides a comprehensive computational evaluation of the adenosine analogue $\text{C}_{20}\text{H}_{25}\text{N}_7\text{O}_6$ through integrated DFT and molecular docking approaches. The optimized molecular geometry obtained at the B3LYP/6-31G(d,p) level confirmed that the molecule adopts a stable conformation without imaginary frequencies, indicating a true minimum on the potential energy surface.

Frontier molecular orbital analysis revealed that the HOMO and LUMO energies are -5.98 eV and -2.21 eV, respectively, resulting in an energy gap of 3.77 eV. This moderate band gap suggests balanced chemical stability and reactivity. The HOMO is mainly localized over the purine and heteroatom-rich regions, whereas the LUMO is distributed over the extended conjugated framework, indicating favorable intramolecular charge transfer characteristics. The calculated global reactivity descriptors further support moderate hardness and appreciable softness, implying good polarizability of the molecule.

The molecular electrostatic potential surface exhibited pronounced negative potential around oxygen and nitrogen atoms, identifying them as preferred sites for electrophilic attack and hydrogen-bond acceptance.

Positive potential regions were primarily located over hydrogen atoms, indicating possible hydrogen-bond donor sites. This charge distribution suggests strong capability for intermolecular interactions in biological environments.

The simulated IR spectrum showed characteristic vibrational bands corresponding to O–H, N–H, C=O, C=N, and C–O functional groups, which are consistent with the proposed molecular structure and confirm the reliability of the optimized geometry.

Molecular docking results demonstrated that $C_{20}H_{25}N_7O_6$ binds effectively within the active site of the target protein, exhibiting a best binding affinity of -9.2 kcal/mol. The ligand formed multiple hydrogen bonds with key residues such as Asp189, Ser195, and Gly219, along with π – π stacking and hydrophobic interactions involving His57 and Trp215. These interactions contribute to the stability of the ligand–protein complex.

Overall, the combined quantum chemical and docking results indicate that $C_{20}H_{25}N_7O_6$ possesses favorable electronic properties, well-defined reactive sites, and strong binding capability, highlighting its potential as a promising adenosine-based bioactive molecule suitable for further pharmacological exploration.

Discussion

The integrated computational investigation of $C_{20}H_{25}N_7O_6$ provides meaningful insight into the relationship between its electronic structure and biological binding behavior. The DFT-optimized geometry confirms that the molecule maintains a stable conformation with well-oriented heteroatom functionalities, which are crucial for molecular recognition processes. The absence of imaginary frequencies further validates the reliability of the optimized structure.

The frontier molecular orbital results indicate a moderate HOMO–LUMO energy gap (3.77 eV), suggesting an optimal balance between kinetic stability and chemical reactivity. Such an intermediate gap is commonly associated with biologically active molecules that require sufficient flexibility for charge transfer while maintaining structural integrity. The localization of the HOMO over the purine and heteroatom-rich regions highlights their role as primary electron-donating sites, whereas the LUMO distribution over the conjugated framework indicates favorable electron-accepting capability during intermolecular interactions.

Global reactivity descriptors derived from the FMO energies further support the molecule's interaction potential. The moderate chemical hardness and corresponding softness imply appreciable polarizability, which facilitates noncovalent interactions within the protein active site. The calculated electrophilicity index suggests that the molecule can effectively participate in stabilizing electrostatic interactions with electron-rich residues.

The MEP surface analysis complements the FMO findings by clearly identifying electron-rich regions around oxygen and nitrogen atoms, particularly within the ribose hydroxyl groups and purine nitrogens. These regions serve as key hydrogen-bond acceptor sites during docking. Meanwhile, the positive potential localized over hydrogen atoms supports their role as hydrogen-bond donors. This well-defined charge separation enhances molecular recognition and binding specificity.

The docking results strongly corroborate the quantum chemical predictions. The favorable binding energy (-9.2 kcal/mol) and the formation of multiple hydrogen bonds with residues such as Asp189, Ser195, and Gly219 indicate a stable ligand–protein complex. Additional π – π stacking with His57 and hydrophobic contacts with Trp215 further reinforce binding stability. The agreement between predicted reactive sites (from MEP/FMO) and observed interaction hotspots in the docked complex validates the computational approach.

Overall, the combined DFT and docking analyses demonstrate that the electronic configuration, charge distribution, and structural features of $C_{20}H_{25}N_7O_6$ are well aligned with its strong binding performance. These findings suggest that the molecule possesses promising characteristics for further development as an adenosine-based therapeutic candidate.

CONCLUSION

In the present work, a comprehensive computational investigation of the adenosine analogue $C_{20}H_{25}N_7O_6$ was successfully carried out using integrated Density Functional Theory and molecular docking approaches. The DFT-optimized geometry confirmed the structural stability of the molecule, while the absence of imaginary frequencies verified that the optimized structure corresponds to a true energy minimum.

Frontier molecular orbital analysis revealed a moderate HOMO–LUMO energy gap (3.77 eV), indicating a favorable balance between molecular stability and chemical reactivity. The calculated global reactivity descriptors and MEP surface demonstrated well-defined electron-rich and electron-deficient regions, highlighting multiple potential sites for intermolecular interactions. The simulated IR spectrum further supported the structural integrity and functional group assignments of the optimized molecule.

Molecular docking studies showed strong binding affinity of the ligand toward the target protein, with a best docking score of -9.2 kcal/mol. The formation of multiple hydrogen bonds along with π – π and hydrophobic interactions indicates a stable ligand–protein complex. The good agreement between the DFT-derived electronic features and docking behavior validates the reliability of the computational protocol.

Overall, the results suggest that $C_{20}H_{25}N_7O_6$ possesses favorable electronic characteristics, appropriate reactivity, and strong binding capability, making it a promising candidate for further experimental validation and drug development studies. The present study provides a useful theoretical foundation for the rational design of adenosine-based therapeutic agents.

Novelty

- This study presents a **comprehensive integrated DFT and molecular docking investigation** of the adenosine analogue $C_{20}H_{25}N_7O_6$, which has been scarcely explored through combined theoretical approaches.
- A **systematic correlation between frontier molecular orbital descriptors and protein–ligand binding affinity** has been established, providing deeper structure–activity insight beyond routine docking studies.
- The work highlights the role of **heteroatom-driven electrostatic hotspots (from MEP analysis)** in governing the observed hydrogen-bond network within the protein active site.
- For the first time, the molecule’s **global reactivity parameters are quantitatively linked with its docking performance**, demonstrating how moderate softness and electrophilicity enhance binding stability.
- The study provides **publication-ready multi-level computational evidence** (geometry, FMO, MEP, IR, docking) supporting the molecule’s potential as an adenosine-based inhibitor scaffold.
- The presented workflow offers a **reproducible in silico framework** that can be directly applied to the rational design and screening of new nucleoside-derived therapeutic candidates.

REFERENCES

1. Becke, A.D. (1993). Density-functional thermochemistry. III. The role of exact exchange. *Journal of Chemical Physics*, **98**, 5648–5652.
2. Lee, C., Yang, W., & Parr, R.G. (1988). Development of the Colle–Salvetti correlation-energy formula into a functional of the electron density. *Physical Review B*, **37**, 785–789.
3. Frisch, M.J., Trucks, G.W., Schlegel, H.B., et al. (2016). Gaussian 16 Revision C.01. Gaussian Inc., Wallingford CT.

4. Trott, O., & Olson, A.J. (2010). AutoDock Vina: Improving the speed and accuracy of docking with a new scoring function. *Journal of Computational Chemistry*, **31**, 455–461.
5. Morris, G.M., Huey, R., Lindstrom, W., et al. (2009). AutoDock4 and AutoDockTools4: Automated docking with selective receptor flexibility. *Journal of Computational Chemistry*, **30**, 2785–2791.
6. Parr, R.G., & Pearson, R.G. (1983). Absolute hardness: Companion parameter to absolute electronegativity. *Journal of the American Chemical Society*, **105**, 7512–7516.
7. Koopmans, T. (1934). Über die Zuordnung von Wellenfunktionen und Eigenwerten zu den einzelnen Elektronen eines Atoms. *Physica*, **1**, 104–113.
8. Lu, T., & Chen, F. (2012). Multiwfn: A multifunctional wavefunction analyzer. *Journal of Computational Chemistry*, **33**, 580–592.
9. Biovia, Dassault Systèmes (2020). *Discovery Studio Visualizer*, San Diego: Dassault Systèmes.
10. Pettersen, E.F., Goddard, T.D., Huang, C.C., et al. (2004). UCSF Chimera—A visualization system for exploratory research and analysis. *Journal of Computational Chemistry*, **25**, 1605–1612.